Conductivity relaxation in ZrF_4-BaF_2-YF_3-NaF glasses

Conductivity relaxation in ZrF$_4$–BaF$_2$–YF$_3$–NaF glasses

M Sural and A Ghosh†

Solid State Physics Department, Indian Association for the Cultivation of Science, Jadavpur, Calcutta 700032, India

Abstract. We have studied the conductivity relaxation of fluoride glasses in the system ZrF$_4$–BaF$_2$–YF$_3$–NaF with NaF content ranging from 5 to 30 mol% in the frequency range 10 Hz–2 MHz and in the temperature range from 300 K to just below the glass transition temperature. The conductivity decreases with the increase of NaF content in the compositions, which is shown to result from the lower and lower decoupling of the F$^-$ ions from the viscous motion of the glassy network. Small values of the stretching exponent are observed for the present glasses and have been associated with the high cooperation between the F$^-$ ions in the conductivity relaxation process.

1. Introduction

Heavy metal fluoride glasses based on ZrF$_4$ are of considerable interest because of their potential uses in ir optical components, ultra-low loss optical fibres, high power laser host materials, sensors, etc [1, 2]. Also these glasses show a very high electrical conductivity for which they can be used as solid electrolytes [3, 4]. The ionic conductivity in the zirconium fluoride glasses arises mainly from the diffusion of fluorine ions [5]. However, zirconium fluoride glasses containing alkali metals as modifiers are fluorine and/or alkali ion conductors, depending on the concentration and nature of alkali ions [6–9]. Some authors have observed the mixed alkali effect in zirconium fluoride glasses [10]. It has been observed that the electrical properties for the zirconium based fluoride glasses containing lithium ions are different from those of the glasses containing sodium ions [6, 7]. The fluoride glasses containing lithium ions have ionic conductivity resulting from the migration of both the F$^-$ and Li$^+$ ions at low concentration of LiF, while at higher concentration of LiF the conductivity results from the motion of Li$^+$ ions only. In contrast, in glasses containing Na$^+$ ions, the conductivity is due to the motion of F$^-$ ions only. That the Na$^+$ ions do not take part in the diffusion process has been confirmed by the ^{23}Na NMR and ^{23}Na-tracer-diffusion results [8, 11]. The objective of the present work is to study the dc conductivity and the conductivity relaxation in the ZrF$_4$–BaF$_2$–YF$_3$–NaF glass system with different NaF content in the temperature range from 300 K to just below the glass transition temperature and in the frequency range 10 Hz–2 MHz.

2. Experiment

The glass samples whose compositions are given in table 1 were prepared using the chemicals ZrF$_4$, BaF$_2$, YF$_3$ and NaF (Aldrich). The appropriate proportions of these chemicals were

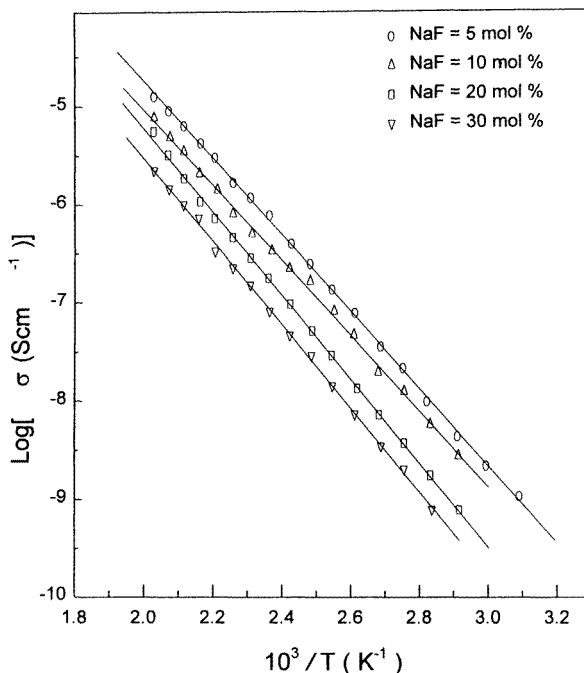† Author to whom all correspondence should be addressed.

Figure 1. Temperature dependence of the dc conductivity for the different glass compositions.

Table 1. Compositions, pre-exponential factor and activation energy for the ZrF_4–BaF_2–YF_3–NaF glasses.

Composition (mol%)				$\log \sigma_0$ (S cm^{-1}) (± 0.01)	W_σ (eV) (± 0.01)	T_g (°C) (± 5)
ZrF_4	BaF_2	YF_3	NaF			
55	30	10	5	3.08	0.76	311
50	30	10	10	2.63	0.74	310
50	20	10	20	3.42	0.83	272
50	10	10	30	2.95	0.82	260

mixed with an excess of ammonium bifluoride. The mixtures were then melted in a covered platinum crucible in an electrical furnace at 800 °C for 10 minutes to avoid much evaporation loss. The melts were finally poured into a preheated aluminium mould. Residual mechanical stresses were removed by annealing the samples at a temperature 50 °C below the glass transition temperature (T_g) which were determined by the differential thermal analysis (DTA) using a heating rate of 20 °C min^{-1}. The amorphous nature of the samples was confirmed by x-ray diffraction. For electrical measurements, gold electrodes were deposited on both surfaces of the polished samples of diameter ∼1.5 cm and thickness ∼0.05–0.01 cm. The gold coated samples were then heat treated at 150 °C for the stabilization of the electrodes. The electrical measurements such as capacitance and conductance of the samples were carried out in the frequency range 10 Hz–2 MHz using a QuadTech RLC meter (model 7600) interfaced with a computer. The measurements were taken in the temperature range from 300 K to just below the glass transition temperature T_g. The dc conductivity was obtained either from the complex impedance plots or from the extrapolation of the frequency independent conductivity. The results of both the calculations agreed very well.
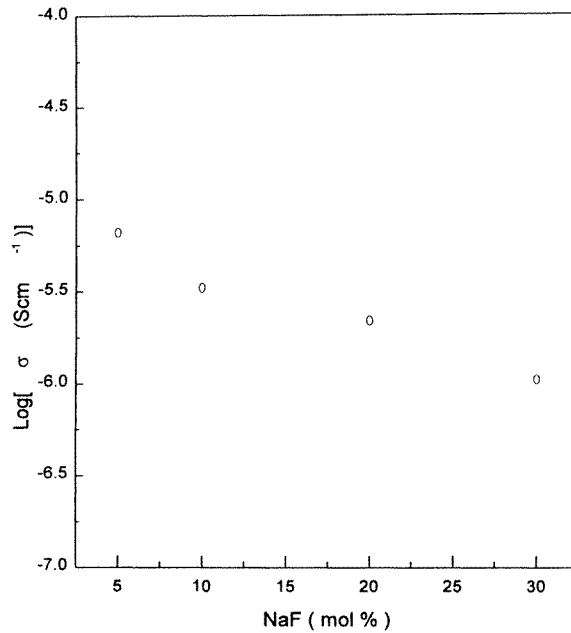
Figure 2. Dependence of the dc conductivity at 473 K (σ_{473}) for the ZrF$_4$–BaF$_2$–YF$_3$–NaF glass on the NaF content in the composition.

3. Results and discussion

The logarithmic dc conductivity as a function of reciprocal temperature for all the glass samples is plotted in figure 1. In all cases, the dc conductivity varies according to the Arrhenius equation $\sigma = \sigma_0 \exp(-W_\sigma/kT)$. The values of the preexponential factor σ_0 and the activation energy W_σ obtained from the least squares straight line fits are shown in table 1 for all glass compositions. The dependence of the dc conductivity at 473 K (σ_{473}) on the NaF content in the glass compositions is shown in figure 2. It is observed that the dc conductivity decreases with the increase of the NaF content in the composition which indicates that the conductivity in these glasses does not arise from the migration of Na$^+$ ions and the F$^-$ ions contribute to the conductivity. These results are supported by the ^{23}Na NMR and ^{23}Na-tracer-diffusion NMR studies [8, 11]. A fraction of the fluorine ions is trapped by the Na$^+$ ions and consequently an increase in the NaF content results in a decrease of the conductivity [12, 13] similar to that in other zirconium glasses containing Na$^+$ ions [9].

We have employed the modulus formalism [14] to analyse the ac conductivity data. In this formalism [14] an electric modulus M^* is defined as the inverse of the complex dielectric constant ε^*:

$$M^* = M'(\omega) + jM''(\omega) = 1/\varepsilon^* = (\varepsilon' - j\varepsilon'')/|\varepsilon^*|^2$$
$$= M_\infty \left[1 - \int_0^\infty \exp(-j\omega t)(d\phi(t)/dt)dt \right] \tag{1}$$

where M' and M'' are the real and imaginary parts of the complex modulus M^*, M_∞ is the inverse of the high frequency dielectric constant ε_∞ and the function $\phi(t)$ gives the time evolution of the electric field and hence the distribution of relaxation time within the material. The frequency dependence of M' and M'' respectively at several temperatures for a particular
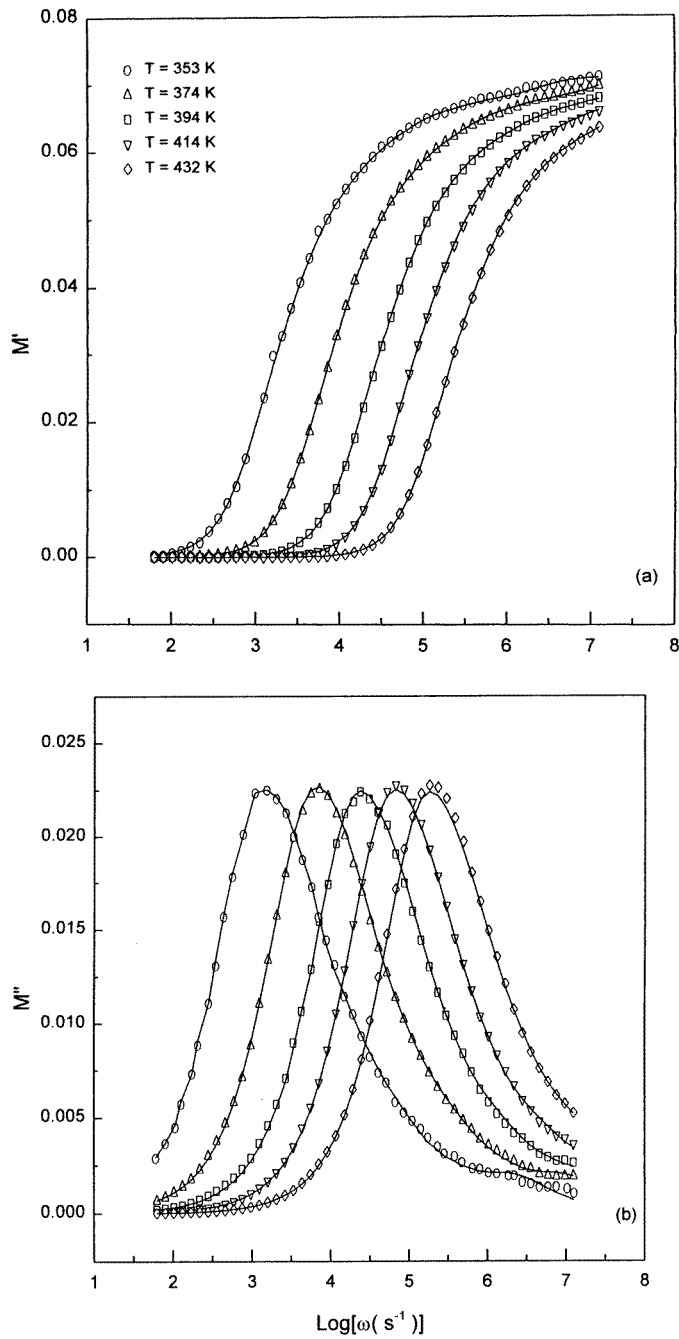
Figure 3. Frequency dependence of M' and M'' at different temperatures for the 50ZrF$_4$–20BaF$_2$–10YF$_3$–20NaF glasses.

glass composition is shown in figures 3(a) and (b). M' shows a dispersion at low frequencies, while at high frequencies it tends to an asymptotic value M_∞. M'' shows an asymmetric maximum (M''_{max}) centred at the dispersion region of M'. It is clear from figure 3(b) that
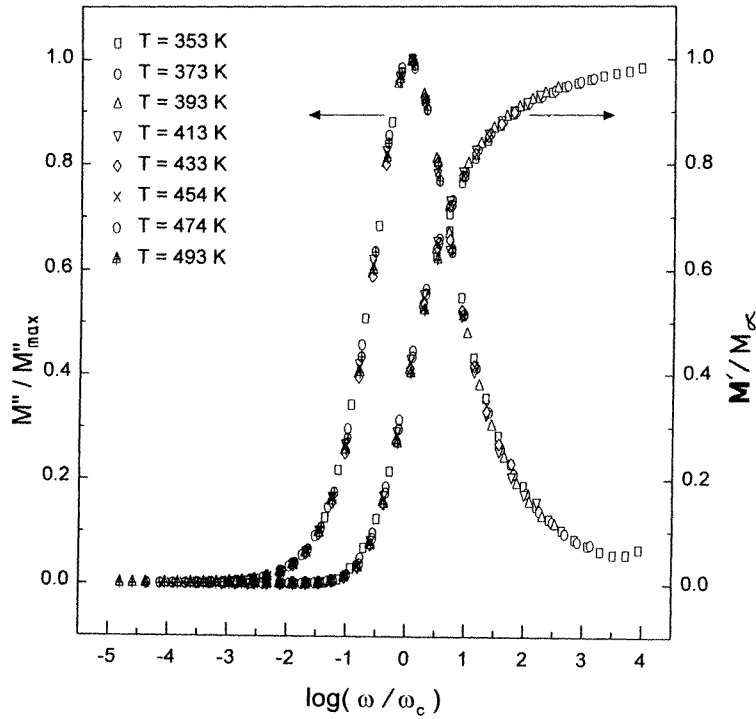
Figure 4. Plot of M'/M_∞ and M''/M''_{max} versus $\log(\omega/\omega_c)$ at different temperatures for the same glass composition as in figure 3.

the maximum of the asymmetric peak shifts towards higher frequencies as the temperature is increased. The frequency ω_c where the maximum in M'' occurs is given by the condition $\omega_c \tau_c = 1$, where τ_c is the most probable conductivity relaxation time and indicates a transition from a short range to a long range mobility at decreasing frequency. Similar effects have also been observed for other glass compositions. A master plot in which M' and M'' are scaled by the M_∞ and M''_{max} respectively and each frequency is scaled by the frequency ω_c is shown in figure 4, which shows that the plots for all temperatures superpose perfectly on a single master curve, implying that the dynamical processes occurring at different frequencies have the same thermal activation energy. The data for M' and M'' for all temperatures were fitted simultaneously to the values obtained from the modulus formalism (equation (1)). In the fitting process, the Kohlrausch–Williams–Watts (KWW) function $\phi(t) = \exp[-(t/\tau_c)^\beta]$ was used [15]. A best fit for a glass composition having 20 mol% NaF is shown in figures 3(a) and 3(b). Other glass compositions also showed similar fits. The values of β and the high frequency dielectric constant ε_∞ obtained from the fits are shown in table 2. It is noted that the values of β are independent of temperature. The temperature dependence of the conductivity relaxation time τ_c obtained from the maximum M'' is shown in figure 5 for all glass compositions. τ_c^{-1} exhibits an Arrhenius behaviour similar to the dc conductivity. The data were fitted in figure 5 to the Arrhenius equation $\tau_c^{-1} = \tau_0^{-1} \exp(-W_c/kT)$. The values of W_c and the pre-exponential factor τ_0 obtained from the fits are shown in table 2 for all glass compositions in agreement with the fluctuation–dissipation theory [16].

The composition dependence of the dc conductivity can be explained on the basis of Angell's criterion. Angell [17, 18] defined the glass decoupling index R_τ by the ratio
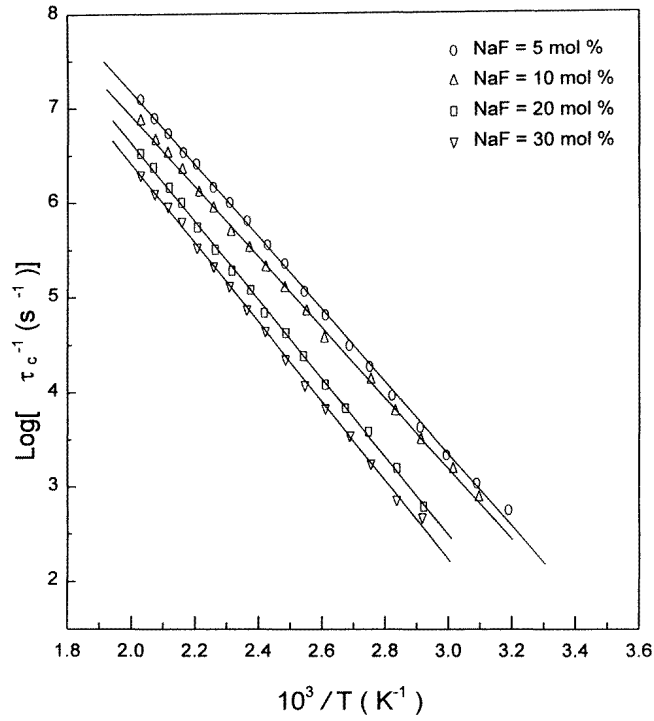
Figure 5. Temperature dependence of the inverse conductivity relaxation time for the same glass compositions as shown in figure 1.
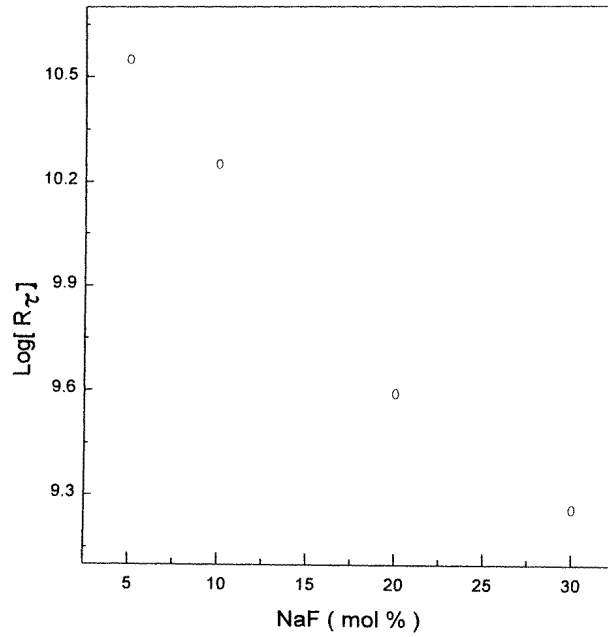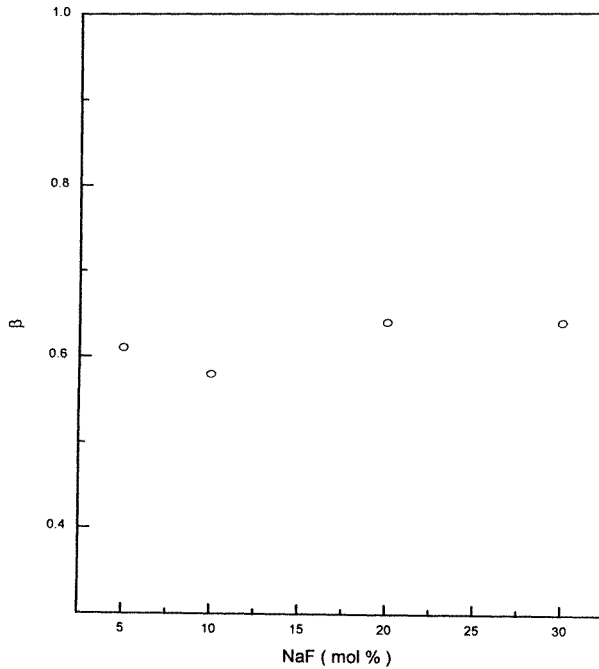

Figure 6. Variation of R_τ with the NaF content in the glass compositions.

Table 2. Different parameters of the studied glasses obtained from the conductivity relaxation model.

Composition (mol% LiF)	W_c (eV) (± 0.01)	$\log \tau_0$ (s)	β	$\varepsilon_\infty = 1/M_\infty$	$\log(R_\tau)$
5	0.76	-14.81	0.61	12.33	10.55
10	0.74	-14.37	0.58	11.05	10.25
20	0.82	-14.91	0.64	14.13	9.59
30	0.82	-14.77	0.64	11.73	9.26

Figure 7. Variation of the stretched exponent β with the NaF content in the glass compositions.

$\langle \tau_s(T_g) \rangle / \langle \tau_c(T_g) \rangle$, where $\langle \tau_s(T_g) \rangle$ and $\langle \tau_c(T_g) \rangle$ are the average structural and conductivity relaxation times at the glass transition temperature T_g. It has been shown that R_τ describes the extent to which motions of the conducting ions in a given glass are decoupled from the viscous motion of the glassy matrix and is consequently related to the ability of the mobile ions to migrate in the glass electrolytes at T_g. We have calculated R_τ by extrapolating the $\log \tau_c^{-1}$ versus $10^3/T$ plots at T_g (figure 5) and assuming the structural relaxation time $\tau_s = 200$ s [18]. The calculated values of R_τ are shown in figure 6 as a function NaF content in the glass compositions. We note that R_τ decreases with the increasing NaF content in the glass compositions, suggesting that the motion of the F$^-$ ions is decoupled less and less from the viscous motion of the glassy network as the NaF content is increased in the compositions and consequently the conductivity decreases.

The composition dependence of the exponent β is shown in figure 7. We note that values of β for all compositions are very small (~ 0.60) and do not vary strongly with composition. It has been suggested that β represents the cooperation between charge carriers in the conductivity relaxation process [19]. The smaller the value of β, the greater is the cooperation between charge carriers. The small values of β observed in the present zirconium fluoride glasses

indicate that the cooperation between F^- ions is high in the relaxation process according to this model.

4. Conclusions

The dc conductivity and the conductivity relaxation of the ZrF_4–BaF_2–YF_3–NaF glass system with varying NaF content have been studied in the temperature range from 300 K to just below the glass transition temperature and in the frequency range 10 Hz–2 MHz. The conductivity decreases with the increase of NaF content in the glass composition due to the trapping of F^- ions by the Na^+ ions. The decrease of the conductivity with the increase of NaF content is also supported by the decrease of the decoupling index. The small values of the stretching exponent for the present glasses arise from the high cooperation between the F^- ions in the conductivity relaxation process.

Acknowledgment

References

[1] Lucas J 1984 *J. Mater. Sci.* **24** 1
[2] Poulain M 1983 *J. Non-Cryst. Solids* **56** 1
[3] Bobe J M, Senegas J, Reau J M and Poulain M 1993 *J. Non-Cryst. Solids* **162** 169
[4] Mai C, Poulain M, Asseiro A M and Johari G P 1989 *J. Non-Cryst. Solids* **113** 94
[5] Reau J M, Senegas J, Aomi H, Hagenmuller P and Poulain M 1985 *Solid State Chem.* **60** 159
[6] Reau J M, Senegas J, Rojo J M and Poulain M 1990 *J. Non-Cryst. Solids* **116** 175
[7] Sural M and Ghosh A 1998 *J. Phys.: Condens. Matter* **10** 10 577
[8] Robe J M, Reau J M, Senegas J and Poulain M 1995 *Solid State Ion.* **82** 39
[9] Robe J M, Reau J M, Senegas J and Poulain M 1997 *J. Non-Cryst. Solids* **209** 122
[10] Pirazzo N I, Mosadegh R and Moynihan C T 1985 *Mater. Sci. Forum* **5** 775
[11] Reau J M, Khant H and Poulain M 1990 *J. Non-Cryst. Solids* **119** 347
[12] Ravaine D, Perera W G and Minier M 1982 *J. Phys. C: Solid State Phys.* **9** 407
[13] Reau J M, Khant H, Poulain M and Hagenmuller P 1991 *Z. Anorg. (Allg.) Chem.* **598/599** 269
[14] Macedo P B, Moynihan C T and Bose R 1972 *Phys. Chem. Glasses* **13** 171
[15] Williams G and Watts D C 1970 *Trans. Faraday Soc.* **23** 626
[16] Ngai L K 1979 *Comments Solid State Phys.* **9** 1
[17] Angell C A 1983 *Solid State Ion.* **9/10** 3
[18] Angell C A 1986 *Solid State Ion.* **18/19** 72
[19] Ngai K L 1992 *J. Physique* **2** 61